

# Mid-infrared doping tunable transmission through subwavelength metal hole arrays on InSb

B. S. Passmore<sup>1,\*</sup>, D. G. Allen<sup>1</sup>, S. R. Vangala<sup>2</sup>, W. D. Goodhue<sup>2</sup>,  
D. Wasserman<sup>2</sup> and E. A. Shaner<sup>1</sup>

<sup>1</sup>Sandia National Laboratories, P.O. Box 5800, Albuquerque, NM 87185, USA

<sup>2</sup>Department of Physics and Applied Physics, University of Massachusetts Lowell, Lowell, MA 01854

\*Corresponding author: [bspassm@sandia.gov](mailto:bspassm@sandia.gov)

**Abstract:** Doping-tunable mid-infrared extraordinary transmission is demonstrated from a periodic metal hole array patterned on n-InSb. The polarization-dependent transmission was measured at room temperature and 77 K. In addition, the extraordinary transmission was measured for incident angles from 0° to 35° in 5° steps. A fundamental resonance shift of ~ 123 cm<sup>-1</sup> (1.4 μm) is observed by varying the doping from 1 x 10<sup>16</sup> to 2 x 10<sup>18</sup> cm<sup>-3</sup>. The calculated transmission resonances were in good agreement with the experimental results. This suggests that InSb semiconductor-based plasmonic structures may be suitable for a variety of tunable mid-infrared device applications.

©2009 Optical Society of America

**OCIS codes:** (240.6690) Surface waves; (250.5403) Plasmonics; (160.1245) Artificially engineered materials; (999.9999) Extraordinary Transmission; (130.3060) Infrared.

---

## References and links

1. T. W. Ebbesen, H. J. Lezec, H. F. Ghaemi, T. Thio, and P. A. Wolff, "Extraordinary optical transmission through sub-wavelength hole arrays," *Nature* **391**, 667-669 (1998).
2. S. M. Williams, A. D. Stafford, K. R. Rodriguez, T. M. Rogers, and J. V. Coe, "Accessing surface plasmons with Ni microarrays for enhanced IR absorption by monolayers," *J. Chem. Phys. B* **107**, 11871-79 (2003).
3. K. D. Moller, K. R. Farmer, D. V. P. Ivanov, O. Sternberg, K. P. Stewart, and P. Lalanne, "Thin and thick cross shaped metal grids," *Infrared Phys. Technol.* **40**, 475-478 (1999).
4. R. Ulrich, "Modes of propagation on an open periodic waveguide for the far infrared," in *Proceedings Symp. Opt. Acoust. Microelectron.*, (Polytechnic Press of the Polytechnic Institute of New York .New York, 1974), pp. 359-376.
5. H. Liu and P. Lalanne, "Microscopic theory of the extraordinary optical transmission," *Nature* **452**, 728-731 (2008).
6. N. Fang, H. Lee, C. Sun, and X. Zhang, "Sub-diffraction-limited optical imaging with a silver superlens," *Science* **308**, 534-537 (2007).
7. N. Fang, Z. Liu, T. J. Yen, and X. Zhang, "Regenerating evanescent waves from a silver superlens," *Opt. Express* **11**, 682-687 (2003).
8. N. Fang and X. Zhang, "Imaging properties of metamaterials superlens," *Appl. Phys. Lett.* **82**, 161-163 (2003).
9. L. Yin, V. K. Vlasko-Vlasov, A. Rydh, J. Pearson, U. Welp, S. H. Chang, S. K. Gray, G. C. Schatz, D. B. Brown, and C. W. Kimball, "Surface plasmons at single nanoholes in Au films," *Appl. Phys. Lett.* **85**, 467-469 (2004).
10. N. E. Glass, A. A. Maradudin, and V. Celli, "Diffraction of light by a bigrating: Surface polariton resonances and electric field enhancements," *Phys. Rev. B: Condens. Matter Mater. Phys.* **27**, 5150-3 (1983).
11. E. Hao and G. C. Schatz, "Electromagnetic fields around silver nanoparticles and dimers," *J. Chem. Phys.* **120**, 357-366 (2004).
12. G. C. Schatz, M. Young, and R. P. V. Duyne, "Electromagnetic mechanism of SERS," in *Surface Enhanced Raman Scattering: Physics and Applications, Springer Topics in Applied Physics*, K. Kneipp, M. Moskovits, H. Kneipp, ed., (Springer, New York, 2006)
13. P. Kambhampati, C. M. Child, M. C. Foster and A. Campion, "On the chemical mechanism of surface enhanced Raman scattering: experiment and theory," *J. Chem. Phys.* **108**, 5013-5026 (1998).
14. J. Coe, K. R. Rodriguez, S. Teeters-Kennedy, K. Cilwa, J. Heer, H. Tian, and S. M. Williams, "Metal films with arrays of tiny holes: Spectroscopy with infrared plasmonic scaffolding," *J. Chem. Phys. C* **111**, 17459-17472 (2007).

15. Y. H. Ye and J. Y. Zhang, "Middle-infrared transmission enhancement through periodically perforated metal films," *Appl. Phys. Lett.* **84**, 2977-9 (2004).
16. K. R. Rodriguez, S. Shah, S. M. Williams, S. Teeters-Kennedy, and J. V. Coe, "Enhanced infrared absorption spectra of self-assembled alkanethiol monolayers using the extraordinary infrared transmission of metallic arrays of subwavelength apertures," *J. Chem. Phys.* **21**, 8672-5 (2005).
17. S. M. Williams, A. D. Stafford, T. M. Rogers, S. R. Bishop, and J. V. Coe, "Extraordinary infrared transmission of Cu-coated arrays with subwavelength apertures: Hole size and the transition from surface plasmon to waveguide transmission," *Appl. Phys. Lett.* **85**, 1472-5 (2004).
18. Y. J. Bao, R. W. Peng, D. J. Shu, M. Wang, X. Lu, J. Shao, W. Lu, and N. B. Ming, "Role of interference between localized and propagating surface waves on the extraordinary optical transmission through a subwavelength-aperture array," *Phys. Rev. Lett.* **101**, 87401-4 (2008).
19. S. A. Maier and H. A. Atwater, "Plasmonics: Localization and guiding of electromagnetic energy in metal/dielectric structures," *J. Appl. Phys.* **98**, 011101-10 (2005).
20. T. Thio, H. F. Ghaemi, H. J. Lezec, P. A. Wolff, and T. W. Ebbesen, "Surface-plasmon-enhanced transmission through hole arrays in Cr films," *J. Opt. Soc. Am. B* **16**, 1743-1748 (1999).
21. P. Hewageegana and V. Apalkov, "Quantum dot photodetectors with metallic diffraction grating: Surface plasmons and strong absorption enhancement," *Physica E* **40**, 2817-2822 (2008).
22. D. Wasserman, E. A. Shaner and J. G. Cederberg, "Midinfrared doping-tunable extraordinary transmission from sub-wavelength gratings," *Appl. Phys. Lett.* **90**, 1911021-3 (2007).
23. O. Manasreh, *Semiconductor heterojunctions and nanostructures*, K. P. McCombs eds., (McGraw-Hill, New York, 2005).
24. E. A. Shaner, J. G. Cederberg and D. Wasserman, "Electrically tunable extraordinary optical transmission gratings," *Appl. Phys. Lett.* **91**, 1811101-3 (2007).
25. H. F. Ghaemi, T. Thio, D. E. Grupp, T. W. Ebbesen, and H. J. Lezec, "Surface plasmons enhance optical transmission through subwavelength holes," *Phys. Rev. B* **58**, 6779-6782 (1998).
26. W. A. Murray, S. Astilean and W. L. Barnes, "Transition from localized surface plasmon-polariton as metallic nanoparticles merge to form a periodic hole array," *Phys. Rev. B* **69**, 1654071-7 (2004).
27. T. Ribaudou, B. Passmore, K. Freitas, E. A. Shaner, J. G. Cederberg and D. Wasserman, "Loss Mechanisms in mid-infrared extraordinary optical transmission gratings," *Opt. Express* **17**, 666-675 (2009).
28. Y. Chen, Y. Wang, Y. Zhang and S. Liu, "Numerical investigation of the transmission enhancement through subwavelength hole array," *Opt. Commun.* **274**, 236-240 (2007).
29. C. Sauvan, C. Billaudeau, S. Collin, N. Bardou, F. Pardo, J. L. Pelouard and P. Lalanne, "Surface plasmon coupling on metallic film perforated by two-dimensional rectangular hole array," *Appl. Phys. Lett.* **92**, 111251-3 (2008).
30. A. Naweed, F. Baumann, W. A. Bailey, Jr., A. S. Karakashian, and W. D. Goodhue, "Evidence for radiative damping in surface-plasmon-mediated light transmission through perforated conducting films," *J. Opt. Soc. Am. B* **20**, 2534-2538 (2003).
31. C. Kittel, *Introduction to Solid State Physics*, S. Johnson, ed., (J. Wiley & Sons Inc., New York 1986).
32. W. Zawadzki, "Electron transport phenomena in small-gap semiconductors," *Adv. Phys.* **23**, 435-522 (1974).
33. E. Litwin-Staszewska, W. Szymanska, and P. Piotrkowski, "The electron mobility and thermoelectric power in InSb at atmospheric and hydrostatic pressures," *Phys. Status Solidi (b)* **106**, 551-559 (1981).
34. W. L. Barnes, W. A. Murray, J. Dintinger, E. Devaux, and T. W. Ebbesen, "Surface plasmon polaritons and their role in the enhanced transmission of light through periodic arrays of subwavelength holes in a metal film," *Phys. Rev. Lett.* **92**, 107401-4 (2004).
35. W. L. Barnes, A. Dereux, and T. W. Ebbesen, "Surface plasmon subwavelength optics," *Nature* **424**, 824-830 (2003).

---

## 1. Introduction

Light incident on arrays of subwavelength holes in metal films has been shown to exhibit transmission exceeding unity when normalized to the unmetallized surface area [1 - 4]. This phenomenon, referred to as extraordinary optical transmission (EOT) is attributed to the excitation of two types of surface waves (SWs) that propagate at the front and rear metallic interfaces, surface plasmon polaritons, and an additional field with quasi-cylindrical behavior [5]. The EOT phenomenon is an easily observable, macroscopic effect, making perforated metal hole arrays an ideal platform for the investigation of tuning mechanisms in plasmonic structures. Other interesting properties and applications that have been investigated include sub-diffraction limit imaging [6], superlensing [7,8], near field scanning optical microscopy [9], high surface electric fields [10,11] for enhanced Raman spectroscopy [12,13] and biological sensors [14].

In the past decade, there have been many advancements in mid-infrared (MIR) based photonic devices. Consequently, the development of EOT in the MIR (3 – 30  $\mu\text{m}$ ) regime has become increasingly important. Although much of the work in the field of EOT has focused on the visible, near-infrared and terahertz regimes, EOT in the MIR range has been shown to have similar characteristics [15-18].

The intensity and EOT resonance peak position is sensitive to the type of metal that the hole array is patterned from [17], the dielectric material adjacent to the metal [19] and the lattice spacing of the holes on the metal array [20]. If the transmission peak resonance can be controlled, EOT based devices can be integrated into infrared photodetectors for enhanced absorption [21] and detection wavelength tunability. Previously, the EOT resonance was tuned 0.147  $\mu\text{m}$  by varying the doping of the underlying GaAs layer [22]. However, our results indicate that a shift of 1.396  $\mu\text{m}$  is possible using an InSb based system. This tunability has the potential to enable a variety of applications including plasmonic spectrometers, tunable filter elements, and beam steering devices.

Due to its low effective mass and high mobility, the plasma frequency of InSb can be pushed into the MIR at lower carrier concentrations compared to other semiconductors such as GaAs. The dielectric function of InSb for different carrier concentrations is displayed in Fig. 1 and was calculated using the Drude approximation, which includes scattering,

$$\epsilon = \epsilon_{\infty} \left[ 1 - \frac{\omega_p^2}{\omega^2 + i\omega\tau^{-1}} \right], \quad \omega_p = \frac{4\pi N e^2}{\epsilon_{\infty} m^*}, \quad (1)$$

where  $\omega_p$  is the plasma frequency,  $N$  is the carrier concentration,  $\epsilon_{\infty}$  is the high frequency dielectric constant of the semiconductor,  $m^*$  is the effective mass in the semiconductor and  $\tau$  is the scattering time [23,24]. The scattering time, or damping term, is used to account for

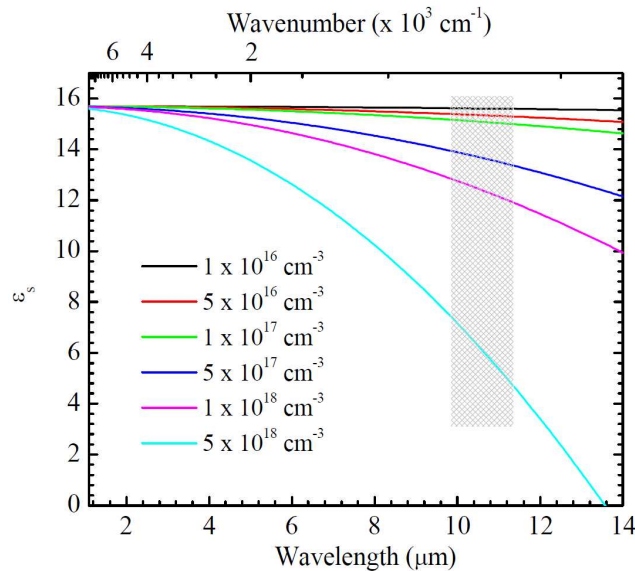


Fig. 1. The dielectric function of InSb for different carrier concentrations. This model includes damping from the scattering time of free electrons.

dissipation of the motion of electrons. As shown in Fig. 1, the difference between the dielectric function between undoped and doped InSb becomes more evident at longer wavelengths for the various carrier concentrations. The shaded region in the plot shows the

wavelength range of the EOT resonant peaks that will be discussed in this study. The normal incident EOT peaks can be roughly defined by the following relation [25],

$$\sqrt{i^2 + j^2} \lambda = a_0 \sqrt{\frac{\epsilon_s \epsilon_m}{\epsilon_s + \epsilon_m}} \approx a_0 \sqrt{\epsilon_s} \text{ for } |\epsilon_m| \gg |\epsilon_s| \quad (2)$$

where  $\lambda$  is the free space wavelength,  $a_0$  is the lattice constant,  $i$  and  $j$  are integers related to the reciprocal lattice vectors  $2\pi/a_0 \mathbf{x}$  and  $2\pi/a_0 \mathbf{y}$ , respectively,  $\epsilon_s$  is the real part of the dielectric function of the semiconductor and  $\epsilon_m$  is the real part of the dielectric function of the metal. From the simpler form, one can see that the EOT resonance can be tuned by changing the dielectric function of the semiconductor. Since the dielectric function of the semiconductor is dependent on the plasma frequency (and thus the material doping), the dielectric function can be altered by control of the semiconductor doping density [3]. While this tuning technique is passive, use of voltage control of the carrier concentration could allow for actively tunable plasmonic devices.

## 2. Experiment

The samples used in this study were grown by molecular beam epitaxy on lightly doped ( $\sim 10^{15} \text{ cm}^{-3}$ ) (111) InSb substrates. The respective carrier concentrations and doped layer thicknesses for the six samples are displayed in Table 1. The carrier concentrations were determined by Hall effect measurements using the Van der Pauw geometry at room temperature.

Table 1. The carrier concentration and doped layer thickness for samples A – F

Sample	Thickness of doped layer (nm)	Carrier Concentration ( $\text{cm}^{-3}$ )
A	NA	0
B	150	$2 \times 10^{17}$
C	150	$5 \times 10^{17}$
D	750	$8 \times 10^{17}$
E	750	$2 \times 10^{18}$
F	2250	$8 \times 10^{17}$

The meshes were patterned using standard processing techniques consisting of photolithography, metal deposition and liftoff. The meshes, consisting of a 60 nm Au film, were designed to have a square lattice of circular holes with a center to center spacing of 2.8  $\mu\text{m}$  and a diameter of 1.4  $\mu\text{m}$ . In order to reduce scattering, the backside of all samples was polished using a chemical mechanical polisher.

The MIR transmission was measured using a Bruker IFS 125HR Fourier-transform infrared spectrometer at room temperature and 77 K. Data was collected with a spectral resolution of  $2 \text{ cm}^{-1}$  and averaged over 200 scans. In addition, the angle- and polarization-dependent transmission was recorded from  $\theta = 0^\circ$ , in increments of  $5^\circ$ , up to  $35^\circ$  for both horizontally and vertically polarized incident light, where “horizontal” and “vertical” polarizations refer to incident light polarized orthogonal and parallel to the axis of rotation, respectively.

### 3. Results

The normal incident transmission spectra at room temperature and 77 K are shown in Fig. 2 for sample A. Here, the  $(\pm 1,0)$  mode can be seen at  $906 \text{ cm}^{-1}$ . When the sample was cooled, the peak transmission not only increased but the transmission range increased as well due to the InSb bandgap shifting to higher energy which resulted in the observation of the  $(1,1)$  and  $(2,0)$  modes.

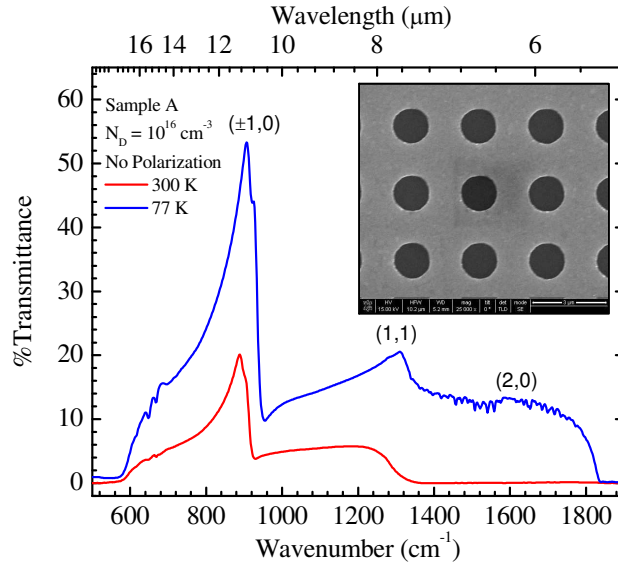


Fig. 2. The normal incident ( $\theta=0^\circ$ ) transmission spectra for Sample A at room temperature and 77 K. The inset shows the scanning electron micrograph of the Au EOT mesh.

The transmission enhancement is primarily due to the reduction of losses at lower temperatures. InSb, due to its narrow bandgap, can have significant thermal generation of carriers at room temperature. While these additional carriers will slightly shift the EOT peak, their dominant effect is from free-carrier absorption in the InSb substrate. A separate study was performed which consisted of measuring the transmission of InSb without a mesh at 77 and 300 K. The transmission at 77 K was more than two times the transmission at room temperature. The 77 K EOT spectra is thus a good indication of the transmission which would be achievable if the substrate were to be removed from the doped epi-grown InSb layer.

The transmission spectra for Sample A ( $N_D = 1 \times 10^{16} \text{ cm}^{-3}$ ) at room temperature, using horizontal polarization, as a function of incident angle is displayed in Fig. 3. When  $\theta = 0^\circ$ , the light is incident normal to the substrate. A polarization-dependent splitting of the EOT resonance is apparent as the incident angle is varied which is due to the angle-dependent in-plane photon wavevector,  $(2\pi/\lambda)\sin\theta$  [1]. The angle-dependent  $(-1,0)$  and  $(+1,0)$  EOT modes are identified by the red and blue dashed lines, respectively. The general angular and polarization dependence of EOT modes for GaAs [22] and quartz [1] substrates have been previously shown to have similar behavior.

In addition to the splitting of the primary transmission peaks, a third peak (green dashed line) is seen in the angular-dependent transmission data. This peak shows weak dispersion,

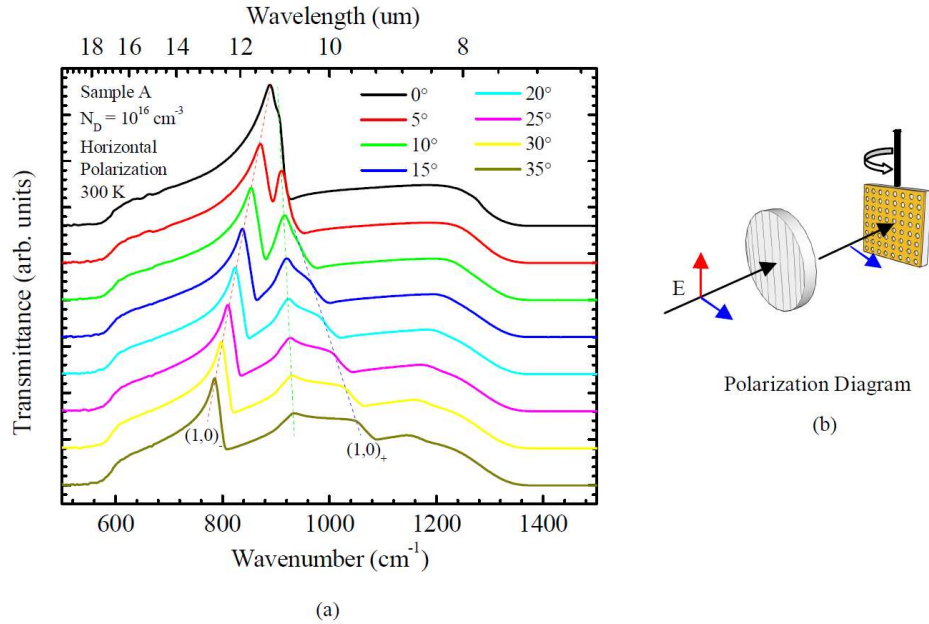


Fig. 3. (a) The transmission spectra for Sample A ( $N_D = 1 \times 10^{16} \text{ cm}^{-3}$ ) at room temperature as a function of the incident angle for angles from  $0^\circ$  to  $35^\circ$  in increments of  $5^\circ$ . The dashed lines were drawn to help distinguish between the peak splitting for the different rotation angles. The higher doped samples have similar characteristics but are shifted to higher wavenumbers. (b) A schematic depicting the light polarized horizontally to the axis of rotation.

shifting only slightly as a function of incidence angle. This phenomenon has been observed in previous studies of the angular dependence of EOT transmission [1, 26, 27]. For mesh thicknesses greater than half the mode wavelength, these angle independent resonances were explained in terms of waveguide resonances that form in the cavity of the mesh [28]. However, in this study the 50 nm mesh thickness is much less than the resonant wavelength. The coupling between SWs in orthogonal directions along a perforated metallic film with rectangular holes was investigated [29]. In that work, it was shown that if light is linearly polarized where  $k_y = 0$ , the  $(0, \pm 1)$  SWs can be stimulated giving rise to the linear splitting and the weak hyperbolic dispersion shown in Fig. 3. It is worth noting that this effect seems to be significantly stronger in our samples when compared to other work [1, 26, 27].

Figure 4 shows the normalized transmission at room temperature for the InSb samples with different carrier concentrations and thicknesses. The transmission spectra were taken normal to the samples without polarization selection. As expected, the transmission blue shifts as the carrier concentration increases due to the free electron contribution to the dielectric constant. By using this mechanism, the transmission in InSb-based EOT structures with the geometries used in this work can be tuned from 9.9 – 11.3  $\mu\text{m}$ .

One drawback to this tuning approach is that for higher doping levels, an increase in linewidth and a decrease in peak intensity were observed due to an increase in losses. The peak transmission at room temperature referenced to free space for sample A was  $\sim 20\%$  whereas the peak transmission for sample E was  $\sim 3\%$ . Thus, large tuning by free carriers comes at the cost of high losses. Radiation damping and other loss mechanisms that contribute to the linewidth are discussed in another study [30]. Figure 4(b) shows that by increasing the thickness of the doped layer and decreasing the carrier concentration, the linewidth of the EOT resonance is reduced. The peak transmission for sample F is  $\sim 7\%$ . Thus, the EOT peak resonance increases for thicker samples with lower doping as well. The comparable EOT

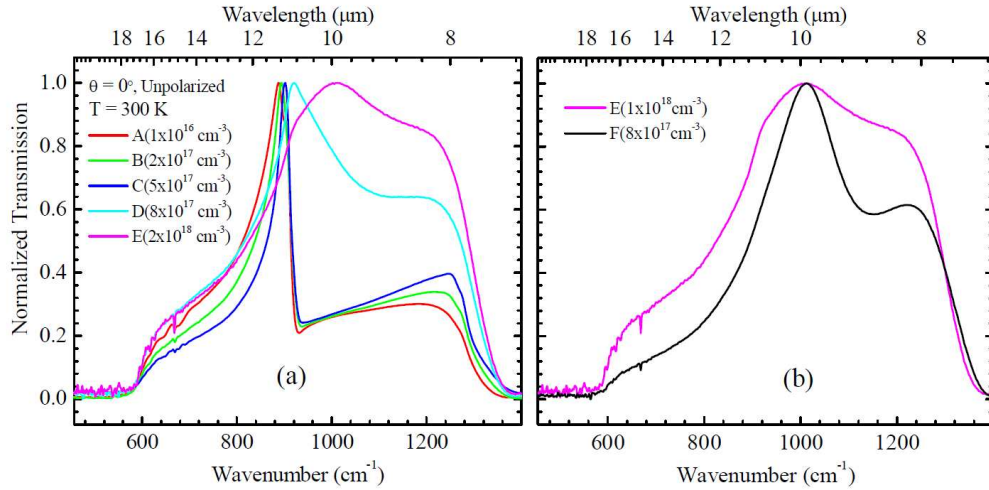


Fig. 4. The normalized transmission at room temperature for samples (a) A – E and (b) E and F. The transmission spectra were taken normal incident to the samples without polarization. A blue shift is observed as the carrier concentration is increased.

peak position shift for sample F is possible due to the larger fraction of the evanescent electric field of the SWs coupling to the thick doped layer.

The EOT resonance for the various doped samples was calculated using Eq. (2) and compared to the experimental results for the  $(\pm 1,0)$  EOT resonance. The comparison is displayed in Fig. 5. A high frequency dielectric constant of 15.7 for InSb was used [31]. In addition, the doping-dependent effective mass and scattering time were taken into account [32, 33]. The average difference between the experimental and theoretical  $(1, 0)$  mode was  $0.559 \mu\text{m}$ . While there is a slight offset between theory and experiment, the trends are well matched. Similarly, previous work has shown that the EOT peak resonance calculations are offset at higher energies compared to experiment [24, 34].

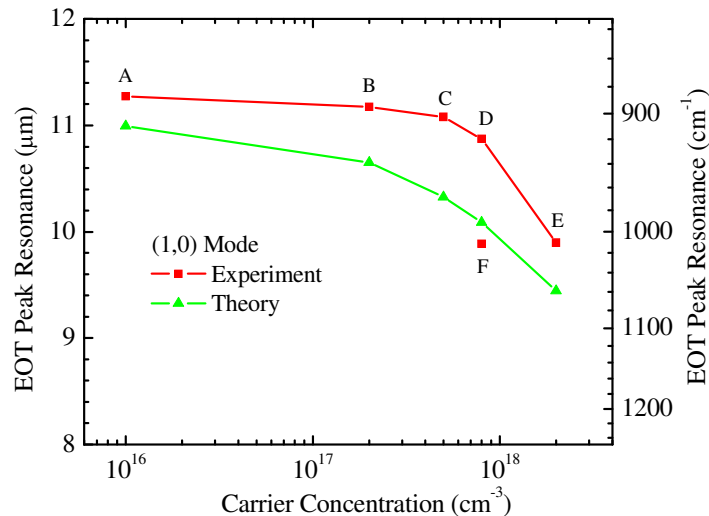


Fig. 5. A comparison between the theoretical and experimental extraordinary optical transmission peak resonances for the  $(1,0)$  mode. A high frequency dielectric constant of 15.7 for InSb was used [29].

It is important to note that the thickness of the doped layers was not taken into consideration when calculating the EOT resonance frequencies. It was assumed that all of the electric field was confined to the doped layer. However, this is not the case as the SW fields fringe roughly  $\lambda/2$  from the surface [35]. If the thickness of the doped layer increased, one would presume that the EOT resonance would be closer to the calculated values. To verify this, the EOT resonance of sample F was compared to the theoretical results. As shown in Fig. 5, the measured EOT resonance of the thick doped sample is very close to the theoretical results. Since more than the full expected shift is observed for 2.25  $\mu\text{m}$ , it is reasonable to assume that the majority of the field is coupled to the doped material. With the difference between experiment and theory for sample F being relatively small, the error can be attributed to the nominal value of the carrier concentration of the grown structure. From Fig. 5, if the doping of Sample F was  $\sim 1 \times 10^{18} \text{ cm}^{-3}$ , the theoretical and experimental data would be in good agreement. Nevertheless, this gives a sufficient measure of the depth to which the mesh fields fringe and demonstrates that the EOT peak resonance can be tuned by not only varying the doping but also the thickness of the doped layer.

#### **4. Conclusion**

Doping-tunable MIR EOT was demonstrated through a subwavelength metal hole array on InSb. A dramatic spectral shift in the primary transmission peak was observed by varying the carrier concentration of the InSb epilayer. The dielectric tuning technique demonstrated here can be applied to a variety of materials and subwavelength grating designs, in addition to the EOT meshes discussed in this paper. The calculated EOT resonances and experimental results showed similar trends suggesting that the EOT can be determined for future designs. Furthermore, if the EOT peak resonance can be actively controlled, plasmonic based devices can be integrated into beam steering devices, on chip optical routers or switches for MIR sensing applications.

#### **Acknowledgment**

This work was performed, in part, at the Center for Integrated Nanotechnologies, a U.S. Department of Energy, Office of Basic Energy Sciences user facility. Sandia National Laboratories is a multi-program laboratory operated by Sandia Corporation, a Lockheed-Martin Company, for the U. S. Department of Energy under Contract No. DE-AC04-94AL85000.